Classification: Biological Sciences

Title: Membrane Proteomics of Phagosomes Suggests a Connection to Autophagy

Author affiliation: Wenqing Shui[1]; Leslie Sheu[2]; Jun Liu[3]; Brian Smart[1]; Christopher J. Petzold[5]; Tsung-yen Hsieh[2], Austin Pitcher[1], Jay D. Keasling*[4,5,7] & Carolyn R. Bertozzi*[1,2,6]

1. Department of Chemistry, University of California, Berkeley, California 94720, USA.

2. Department of Molecular and Cell Biology, University of California, Berkeley, California 94720, USA.

3. Biological Products Division, Bayer HealthCare LLC, Berkeley, California 94701, USA.

4. Departments of Chemical Engineering and Bioengineering, University of California, Berkeley, California 94720, USA.

5. Physical Bioscience Division, Lawrence Berkeley National Laboratory, Berkeley, California 94720, USA.

6. Molecular Foundry, Lawrence Berkeley National Laboratory, Berkeley, California 94720, USA.

7. Joint BioEnergy Institute, Emeryville, California 94720, USA.

***Corresponding authors:**

C.R.B., crb@berkeley.edu; J.D.K., keasling@berkeley.edu.

Manuscript information: 19 pages, 7 figures, 2 supporting figure, 1 table, 4 supporting tables; abstract= 143 words

Abstract

Phagocytosis is the central process by which macrophage cells internalize and eliminate infectious microbes as well as apoptotic cells. During maturation, phagosomes containing engulfed particles fuse with various endosomal compartments through the action of regulatory molecules on the phagosomal membrane. In this study, we performed a proteomic analysis of the membrane fraction from latex bead-containing (LBC) phagosomes isolated from macrophages. The profile, which comprised 546 proteins, suggests diverse functions of the phagosome and potential connections to secretory processes, toll-like receptor signaling and autophagy. Many identified proteins were not previously known to reside in the phagosome. We characterized several proteins in LBC phagosomes that change in abundance upon induction of autophagy, a process that has been previously implicated in the host defense against microbial pathogens. These observations suggest crosstalk between autophagy and phagocytosis that may be relevant to the innate immune response of macrophages.

Introduction

Phagosomes are specialized membrane-bound organelles generated in phagocytic cells such as macrophages, neutrophils and dendritic cells. Their purpose is to internalize foreign particles, microorganisms or apoptotic cells in order to mount an immune response or maintain tissue homeostasis (1). The nascent phagosome undergoes a complex maturation process involving sequential fusion with endosomal compartments. Once mature, the phagosome degrades its constituents and facilitates antigen presentation in a highly controlled manner (2-4). Insight into the biogenesis and immunity-related functions of the phagosome has come from analysis of its protein contents. Previous studies have profiled the proteomes of latex bead-containing (LBC) phagosomes in cell lines from mice (5-7) and *Drosophila* (8), as well as *Dictyostelium discoideum* (9) and *Entamoeba histolytica* (10). These elegant studies have contributed to our understanding of phagosome maturation (6, 9) and modulation by cytokines (7). However, because the entire contents of the phagosomes were sampled, abundant proteins such as soluble lysosomal hydrolases might have obscured lower abundance membrane-bound regulatory proteins or signaling factors.

In order to identify such lower abundance species, we enriched integral and peripheral membrane proteins from macrophage LBC phagosomes by organelle sub-fractionation before carrying out a large-scale proteomic analysis. The 546 proteins identified in our study included 49 membrane receptors, 64 transporter proteins, 107 regulators of vesicle and protein trafficking (including GTPases), and many components from cellular machineries other than phagosomes. One of the new proteins exclusively found in our study, LC3-II, is considered a marker of autophagy activity. Its presence in phagosomes suggests an unexplored linkage between autophagy and phagocytosis. Apart from its housekeeping role in maintaining cellular homeostasis, autophagy has been implicated in cancer, neurodegerative disorders, aging and more recently, immunity against intracellular microbes (11-13). We show here that LC3-II levels in phagosomes are modulated by autophagic activity, along with several other proteins not previously associated with autophagy. These results underscore the power of membrane-specific phagosomal proteomics for identifying new processes that this organelle may engage in.

Experimental Procedures

Antibodies - The rat anti-LAMP1 mAb, mouse anti-GM130 mAb, mouse anti-calnexin mAb, mouse anti-HSP 60 mAb and mouse anti-JAK1 were from BD Biosciences. The goat anti-EEA1 pAb, rabbit anti-vacuolar ATPase pAb, and goat anti-cathepsin D pAb were from Santa Cruz Biotechnology. The rabbit anti-VAMP4 pAb and rabbit anti-actin pAb were from Abcam. The rabbit anti-LC3B pAb and mouse anti-tubulin mAb were from Sigma. The mouse anti-Transferrin receptor mAb was from Zymed Laboratories. The rabbit anti-TLR7 pAb was from Cell Signaling. The rat anti-HA mAb (clone 3F10) was from Roche Applied Science. All secondary Abs for Western blots were from SouthernBiotech.

Phagosome Isolation and Membrane Fractionation – The murine macrophage cell line J774A.1 was cultured as a monolayer in DMEM medium supplemented with 10% fetal bovine serum, 100 units/mL penicillin/streptomycin, and 2 mM L-glutamine (GIBCO). Another macrophage cell line, RAW 264.7 stably expressing HA tagged-TLR9, was cultured in RPMI-1640 (GIBCO, formulated with HEPES and glutamine) supplemented with 10% fetal bovine serum and 100 units/mL penicillin/streptomycin. Both cell lines were incubated with 0.8 μm blue-dyed latex beads (Sigma) for 1 h at a multiplicity of infection at 50:1 to generate phagosomes, washed with ice-cold PBS and incubated in new medium for 1 h. Each cell internalized 5-10 microbeads. After gentle cell lysis using a Dounce homogenizer to reach 90-95% breakage, the bead-containing phagosomes were isolated on a sucrose gradient described by Desjardins and coworkers (14) . The phagosome band on top of the sucrose gradient (10%) as well as three additional bands (fractions 1, 2, 3) at the gradient interfaces beneath (25%, 35% and 60%) were collected [Supporting information (SI) Fig. S1). Fractions 1, 2 and 3 were subjected to TCA-mediated protein precipitation followed by acetone wash, then centrifuged to acquire protein pellets. The pellets were dissolved in 4% SDS in 50mM Tris-HCl buffer (pH 8.0) by vortexing on an agitator (Eppendorf) at 1400 rpm for 1 h at 20 °C. Protein solutions obtained from the supernatant after centrifugation (14000 rpm X 15 min at 4 °C) were used for immunoblots.

The phagosome fraction was resuspended in PBS containing protease inhibitor cocktail (Calbiochem) and washed by ultracentrifugation. The pelleted phagosomes were either resuspended in 4% SDS buffer for total protein extraction as described above or subjected to further fractionation for enriching membrane-bound proteins using the following protocol. Washed phagosomes were

resuspended in 0.2 M Na_2CO_3 (pH 11.0) and the organelle membranes were disrupted by 5-7 passages of the suspension through a 25G syringe needle. The resulting sample was left on ice for 30 min before the membrane fraction was pelleted by centrifugation for 45 min at 200,600 x g at 4 °C. Luminal soluble proteins from the supernatant were precipitated and redissolved similarly to the proteins in fraction B1-B3 in order to obtain a concentrated protein mixture. The phagosomal membrane pellet was directly resuspended in 4% SDS buffer for protein extraction as described above. All the protein extracts were diluted two-fold with 50 mM Tris-HCl buffer before the protein concentration was determined by the BCA assay (Piece).

SDS-PAGE and In-gel Digestion - In order to profile membrane-bound components of macrophage phagosomes, 35 µg of membrane-extracted proteins were separated by SDS-PAGE (4-12%, Bio-Rad). The entire Coomassie-stained gel was cut into 23 consecutive bands and the gel slices were subjected to in-gel digestion via a standard procedure described by Gu *et al*. (15) Notably, the phagosome isolation, membrane fractionation, protein separation and digestion were repeated to acquire duplicate proteome samples for analysis using two types of mass spectrometers as described below.

Protein Identification by LC-MS/MS and Data Analysis - The in-gel digest of each band was further separated by liquid chromatography and analyzed by electrospray ionization tandem MS. In brief, all the peptide digests were first dried on a speed vacuum and reconstituted in 20 µl of 0.1% formic acid (FA). Each sample was injected onto a LC Packings PepMap100 trapping column (0.3 mm × 5 mm). Reversed-phase separation was completed on a LC Packings PepMap C_{18} column (3 µm, 0.075 × 150 mm) at a flow rate of 200 nl/min using buffers 2% CH_3CN, 0.1% FA (A) and 80% CH_3CN, 0.1% FA (B). The gradient was 0-30% B in 100 min, 30-100% B in 10 min, and 100% B for 10 min. The eluted peptides were injected into a given type of nanoESI-MS/MS instrument for protein identification.

To maximize the membrane proteome recovery, we prepared biological replicates to be analyzed by either ESI Q-TOF Mass Analyzer (QSTAR® Hybrid Quadrupole TOF, Applied Biosystems) or ESI Linear Ion Trap Mass Analyzer (LTQ, Thermo Inc.) in a data-dependent acquisition mode. The QSTAR system carried out a survey scan in the mass range of *m/z* 350-1600. Up to three precursor ions exceeding the peak intensity of 30 ion counts were selected automatedly for fragmentation in MS/MS analysis. Product ions were detected in the range of *m/z* 70-2000. The instrument was calibrated and

tuned following each batch of six injections. The major parameters for LTQ data acquisition were: scan range, 400-2000 m/z; precursor ion selection, 6 most abundant peaks per scan for MS/MS; minimal ion signal, 500; and normalized collision energy, 35.0 %.

LC-MS/MS data collected from both instruments were analyzed using the Mascot (version 2.1.03, Matrix Science, UK) search engine on a non-redundant International Protein Index (IPI) mouse database (version 3.24 >50,000 entries). Up to one missed trypsin cleavage was allowed, and carboxyaminomethylation and Met oxidation were selected as a fixed and variable modification, respectively. The mass tolerance for an individual set of data is: for QSTAR data, parent mass error 0.1 Da, fragment mass error 0.15 Da; for LTQ data, parent mass error 2.0 Da, fragment mass error 0.8 Da. The filter criteria for high-confidence protein IDs included 1) above 98% probability; 2) minimal peptide ion score of 20; 3) at least two unique peptide sequences for each protein hit (to eliminate homologous proteins identified with the same set of peptides). The false positive rate of the aforementioned filter criteria was below 1.6%, estimated by using an individual reversed (decoy) sequence database of the entire mouse genome as described previously (16). In brief, the false positive rate was calculated by dividing the number of decoy hits by the number of hits acquired in search using the forward sequence database.

Each protein ID with an IPI accession number was then assigned a major cellular function by using the online tool GO-Getter (http://bmf2.colorado.edu/go-getter/help.psp) based on Genome Ontology (GO) terms. Unassigned entries were searched against Swiss-Prot and NCBI for functional annotation. The number of transmembrane helices in each protein was predicted using TMHMM online program (http://www.cbs.dtu.dk/services/TMHMM/).

Autophagy Induction by Starvation and Drug Treatment for Biochemical Study– Autophagy was induced by amino acid and serum starvation. J774 cells were washed three times with PBS and incubated in the starvation medium Earle's balanced salts solution (EBSS, Invitrogen) for 2 h at 37 °C (17). Vinblastine (Sigma) was added to EBSS at 50 μM to accumulate autophagosomes by blocking their fusion with endosomes/lysosomes (18). Alternatively, protease inhibitors E64 (10 μM) and pepstatin A (2 μM) were added to EBSS to prevent degradation of autophagosomal components in the mature autophagolysosomes. 3-Methyladenine (Sigma) was added to EBSS at 10 mM for autophagy inhibition

(19). Cells were harvested after 2 h starvation in the presence or absence of a particular drug. We also performed subcellular fractionation from autophagy-induced J774 cells. Briefly, the cells were incubated with latex beads diluted in warm medium at a multiplicity of infection of 50:1 for 1 h. After washing the cells three times with PBS to remove free beads, we incubated them with EBSS in the presence or absence of a particular drug for another 2 h. Finally, the cells were lysed and phagosomes along with three additional subcelluar fractions were isolated in the same manner described earlier.

Autophagy Induction for Live Cell Imaging - We used a macrophage cell line stably expressing GFP-fused LC3 (kindly provided by Patrick Fitzgerald, St Jude's Children's Research Hospital, Memphis, TN) to investigate LC3 trafficking during autophagy regulation. Cells were seeded on 8-well Nunc Lab-Tek Chambered Coverglass microscopy slides (Fisher) 20 h before imaging experiment. After incubation with latex beads (3.0 μm microspheres, Polysciences) for 1 h and extensive washes, the cells were treated with chloroquine (50 μM) or 3-MA (10 mM) for 2 h. During the final 15 min, LysoTracker Red DND-99 (Molecular Probes) was added at 100 nM. Cells were washed with PBS and treated with 15 μg/mL Hoechst 33342 (Molecular Probes) in PBS for 2 min. Finally, the live cells were rinsed and imaged using a Zeiss 200M epifluorescence microscope. All images were deconvolved using the nearest neighbor deconvolution algorithm in the instrument software Slidebook 4.2 (Intelligent Imaging Innovations).

Immunoblots – The total lysate from starved and drug-treated cells was obtained by sonicating cells in 2% SDS, 50mM Tris-HCl buffer (pH 8.0) with protease inhibitor cocktail (Calbiochem). After centrifugation, the supernatant was collected and the protein was quantified by the BCA assay. Protein extracts were separated by SDS-PAGE (4-12% for most experiments, except using 12% gel for LC3 detection) and analyzed by Western blots with relevant antibodies. 3 ug of each subcellular fraction was loaded for detection of VAMP4, LC3 and JAK1, while 7 ug was loaded for TLR7 and TLR9 detection. All the total cell lysates were loaded at 15 ug. Phagosomal proteins from starved and drug-treated cells were extracted in the same manner as those from normal cells. Silver stain or protein controls were used to confirm equal protein loading.

Results and discussion

Phagosome Isolation and Membrane Fractionation

Fig. 1 illustrates our procedure for integrating subcellular fractionation techniques with the proteomic platform. We applied the method of Desjardins and coworkers for phagosome isolation (14). Briefly, latex beads were internalized into macrophages and the latex bead-containing (LBC) phagosomes were isolated by flotation on a sucrose gradient. Phagosomes isolated in this manner have been shown to be devoid of major contaminants (14, 20) and retain critical functional capabilities such as sequential fusion with endocytic vesicles (21) and microbicidal activity (22). Using radiolabeling and proteomic analysis, Desjardins and coworkers have previously estimated the potential contamination of LBC phagosomes to be below 5% (8). The first proteomic study of LBC phagosomes using this method identified about 140 proteins. Not surprisingly, many of the observed proteins were highly abundant lysosomal hydrolases from the lumen of the vesicle.

In order to favor the recovery of integral or peripheral membrane proteins, which are at relatively low abundance, we lysed the phagosome pellet in sodium carbonate to release luminal proteins. The most loosely-bound membrane-associated components were then depleted by a second centrifugation. It should be noted that several soluble proteins known to be transiently associated with phagosome membranes participate in vesicle traffic and signaling (such as the Rab family) (23-25). In an effort to retain some of these functionally significant proteins, we refrained from extensive subsequent washing of the membrane fraction. The resulting insoluble pellet was resuspended in concentrated detergent (4% SDS) to solubilize the residual proteins before separation by SDS-PAGE and identification by LC-MS/MS. Enrichment of unique proteins in the purified phagosomal membrane fraction compared to other fractions was confirmed by SDS-PAGE (Fig. S1).

In order to verify the purity of isolated phagosomes and their membrane fractions, we probed for the presence of known cellular organelle markers. GM-130 (Golgi-resident), Calnexin (ER-resident) and HSP-60 (mitochondria-resident) were detected only in non-phagosome fractions whereas the lysosomal-associated membrane protein-1 (LAMP1) was clearly present in the phagosome fraction, as expected from the process of phagosome-lysosome fusion (Fig. 2*A*). In the absence of latex beads, LAMP1 was not observed in the corresponding fraction obtained by centrifugation, thus confirming its association with phagosomal membranes.

We next evaluated the composition of the phagosomal membrane preparation with respect to membrane-associated versus soluble proteins. Western blot analysis demonstrated that three known membrane markers of endosomal compartments, early endosomal associated protein (EEA1), LAMP1 and transferrin receptor (TfR), were more abundantly represented in the membrane extract than in the soluble luminal fraction (Fig. 2*B*). All three endosomal markers were also observed in other subcellular fractions that include endogenous endocytic vesicles. In contrast to membrane markers, a significant portion of the soluble phagosomal protease cathepsin D (CatD) was released into the lumen fraction. However, this luminal protein was also observed as a contaminant in our membrane fraction. Thus, although our method enriches membrane-bound proteins considerably, the membrane fraction is not free of soluble contaminants.

Identification of Phagosomal Membrane-bound Proteins and Functional Categorization

Two types of mass spectrometers (Q-TOF and linear ion trap) were utilized to identify phagosomal membrane-bound proteins prepared in biological duplicates. The raw MS/MS data acquired from the two instruments were searched by a single engine (Mascot) and a stringent set of filter criteria were applied to select high-confidence protein IDs (see Methods for filter definition). A total of 546 non-redundant IDs were generated after removing duplicate hits from the two datasets acquired using the different instruments. The details of protein identifications are listed in Table S1. Interestingly, when we compared our dataset with that from the recent study conducted by Foster *et al.* (6), which identified 505 proteins from entire phagosomes of a different mouse macrophage cell line (without membrane fractionation), 318 IDs were exclusively found in our dataset and 277 IDs were unique hits revealed by Foster's experiment (Fig. 3*A*). All of the 546 proteins identified in our analysis were categorized into 14 major classes according to specific cellular processes or functions annotated in public databases (Fig. 4 and Table S3). We also listed these proteins in order of relative abundance as indicated by their ID score and number of identified peptides (Table S4).

Table S2 highlights unique proteins identified in the previously reported phagosomal proteome dataset as well as the one we acquired here, with a summary of their molecular weights (MW) and number of predicted transmembrane helices (TMHs) based on primary sequences. These data are

presented graphically in Figs. 3*B* and *C*, respectively. The histogram of MWs shows an overall similar distribution profile, though our dataset contains slightly more IDs above 40 kD than the previously reported phagosomal proteomic dataset (6). We found 198 hits with more than one predicted TMH, which constitutes 36% of the entire phagosomal proteome in our analysis. By comparison, 27% of the phagosomal proteome reported by Foster was predicted to comprise transmembrane proteins (6), and a proteomic profile of *Drosophila* phagosomes estimated that value at 19.8% (8). Furthermore, proteins with more than one TMH were represented at higher frequency in our unique dataset compared to unique proteins in the previously reported datasets. Among our uniquely-identified proteins are ion channel and solute carrier proteins, a class of predicted transmembrane proteins with unknown function, as well as members of the vesicle-associated membrane protein (VAMP) family (Table S2). Overall, comparison of the identity and physical properties of proteins from the two datasets indicates that: (1) membrane enrichment allows for discovery of more transmembrane proteins without significantly altering MW distribution, and (2) two separate experiments with different cell lines using different mass spectrometers generated many unique IDs.

Validation of Newly Identified Phagosomal Components

We selected several proteins for further validation by immunoblotting. Some were previously revealed in the earlier study by Desjardin (5), thus providing a measure of further validation, while others were newly identified in this study. As shown in Fig. 5, VAMP4, toll-like receptor (TLR)7 and TLR9, Janus kinase 1 (JAK1), and microtubule-associated protein 1 light chain 3 (LC3) were enriched in the phagosomal membrane fraction compared to other subcellular fractions or total cell lysate. Foster *et al.* also identified VAMP4 in macrophage phagosomes by mass spectrometry (6), and certain TLRs were similarly identified by Desjardin in a recent study of macrophage activation by cytokines (7). By contrast, JAK1 and LC3, which participate in immune signaling and autophagy, respectively, had not been identified previously in phagosomes. The functional implications of each of these findings are summarized below.

VAMP4 is a member of the soluble N-ethylmaleimide-sensitive factor attachment receptor (SNARE) protein family that mediates intracellular membrane trafficking and fusion (26). VAMP4 is

associated with the trans-Golgi network (TGN) and immature secretory granules (27) and is known to mediate trafficking of the sorting and recycling endosomes (28). The protein has not been directly implicated in phagocytosis, but enrichment of VAMP4 on LBC phagosomes suggests a potential role in this pathway. In addition to VAMP4, many other proteins annotated with relevance to "Vesicle and protein trafficking" (Table S3), such as VAMP3, t-SNARE-interacting proteins and Sec family members, were newly identified in our study. Their potential contribution to the biogenesis or functions of macrophage phagosomes is an interesting future avenue of investigation.

The TLR family plays a critical role in innate immunity by recognizing a diverse range of microbial components (29). Several TLR members were identified in our study, as summarized in Table 1. TLR3, 7 and 9 are intracellular receptors that sense bacterial or viral nucleic acids in endosomal compartments, but their relation to phagocytosis is not well understood. Using proteomic techniques, Desjardin found these three TLRs to be upregulated within macrophage phagosomes upon IFN-γ treatment (7). Surprisingly, an uncharacterized TLR member, TLR13, was identified in our study and its relative abundance (estimated by normalizing the number of identified peptides with the theoretical protein size (30)) was significantly higher than all of the other TLRs found in phagosomes (Table 1). This observation suggests that further exploration of the role of TRL13 in phagocytosis is warranted.

JAK1, a protein tyrosine kinase, is known to associate with the cytoplasmic tail of cytokine receptors and plays a crucial role in initiating JAK/STAT signaling for enhancing microbial killing, antigen presentation, and inflammatory cytokine production (31). Fluorescence microscopy analysis a JAK1-YFP fusion showed the protein to be localized primarily at the plasma membrane (32). However, we identified native JAK1 in the phagosomal membranes of macrophage cells, suggesting a possible role in immune defense or other functions of this organelle.

Finally, LC3 piqued our interest because it is a widely used marker and essential component of the autophagy machinery. Upon the induction of autophagy, the 18-kD cytosolic precursor LC3-I is cleaved at its C-terminus and conjugated to phosphotidylethanolamine, generating a 16-kD form termed LC3-II (33). Lipid-modified LC3-II integrates into the membrane of autophagosomes and undergoes either recycling or degradation when autophagosomes fuse with late endosomes (13). Interestingly, we observed the specific enrichment of LC3-II on LBC phagosomal membranes, while both forms of LC3

were observed in the total cell lysate (Fig. 5). It is unlikely that LC3-II found in LBC phagosomes came from contamination of the preparation with autophagosomal membranes. LBC phagosomes are known to be devoid of double-membrane vacuoles (a key feature of autophagosomes) and other major cellular compartments (5, 8, 14, 20). The finding of LC3-II in LBC macrophages prompted us to explore the link between phagosomal components and autophagy more closely.

Regulation of Phagosomal Components upon Autophagy Induction

Autophagy is a fundamental homeostatic process that enables cells to clean up or turn over portions of their own cytoplasm, mainly to obtain nutrients or to remove damaged organelles or toxic macromolecules (34). Autophagy functions are broadly associated with the control of cell development, suppression of tumorogenesis, prevention of neurodegeneration, and the immune response (11-13). Upon the initiation of autophagy, discrete portions of the cytoplasm are sequestered into a membrane-enclosed vacuole termed the autophagosome. The cytosolic components or organelles trapped within a nascent autophagosome are eventually degraded after its fusion with late endosomes (13).

To assess the relationship of phagosomal LC3-II and autophagic activity, we induced autophagy by nutrient starvation (35) in the presence and absence of pharmacological modulators and monitored LC3-II levels within LBC phagosomes by Western blot analysis. Vinblastine was used to accumulate autophagosmes by preventing their fusion with endosomal compartments, and protease inhibitors were employed to accumulate autophagosomal components by preventing their degradation within autolysosomes (17). Further, we employed 3-methyladenine (3-MA), which blocks class III PI3Ks, as an inhibitor of the autophagy pathway (19, 36). The effectiveness of our phagosome purification from these autophagy-regulated cells was verified by the observation of similar patterns of organelle marker distribution in subcelluar fractions between control and drug-treated cells (SI Fig. S2).

As expected, LC3-II from total cell lysates of starved macrophages was more abundant in the presence of vinblastine or protease inhibitors than in their absence (Fig. 6*A*), consistent with the accumulation of autophagsomes. We also found LC3-II levels in LBC phagosomes to be elevated in the presence of vinblastine and protease inhibitors. Since LC3-II is predominantly associated with autophagosomes in non-phagocytic cells, and vinblastine blocks fusion of autophagosomes with

endocytic compartments (33, 37), we suspect that LC3-II was directly transferred from autophagosomes to LBC phagosomes. Consistent with this hypothesis, 3-MA treatment, which inhibited autophagosome formation, reduced LC3-II levels within LBC phagosomes (Fig. 6*A*).

Fluorescence microscopy of RAW cells stably expressing GFP-LC3 was employed to confirm the enrichment of LC3 on phagosome membranes during autophagy induction. We observed a distinct translocation of GFP-LC3 to the outermost ring of latex beads engulfed by macrophages treated with chloroquine-containing medium or starvation buffer (Fig. 7). These LC3-enriched phagosomes underwent successful fusion with lysosomes to become acidic vacuoles as indicated by LysoTracker stain (Fig. 7). In contrast, 3-MA treatment abolished both GFP-LC3 recruitment to phagosmes and LysoTracker staining due to inhibition of PI3K, an essential factor for autophagy induction as well as H^+-ATPase complex assembly (38). Notably, we also observed diffuse LC3 staining around a portion of LBC phagosomes in control cells (Fig. 7), suggesting a low level of endogenous autophagic activity. This observation was consistent with our previous identification of LC3 in phagosome membranes from unstimulated macrophages using the proteomic approach.

Similarly to LC3-II's response to autophagy activity, the amount of VAMP4 in LBC phagosomes increased drastically when autophagosomes were accumulated, and decreased during inhibition of autophagy (Fig. 6A, lane 6-10). This trend suggests trafficking of VAMP4 between the two types of phagocytic compartments. We attributed the change of VAMP4 levels in phagosomes to intracellular translocation because the total cellular level of this protein was observed to be constant (Fig. 6A, lane 1-5). The specific role of VAMP4 in either phagocytosis or autophagy has not been elucidated and would be an intriguing subject to pursue. JAK1, another newly identified phagosomal component, did not show a dramatic change of total expression or subcellular distribution upon autophagy induction (Fig. 6A).

We further probed the response of other identified phagosomal components – the endosomal markers EEA1, transferrin receptor (TrR), LAMP1 and the lysosomal hydrolase cathepsin D (CatD), to autophagy induction. None of these proteins were found upregulated in phagosomes upon autophagy activation, nor were their overall cellular expression levels significantly altered (Fig. 6*B*). This result suggests that LC3-II and VAMP4 are specifically regulated in response to autophagy. We also noticed that the relative levels of the endosomal and lysosomal markers within phagosomes differed from one

another, particularly upon treatment of macrophages with vinblastine (lane 9 in Fig. 6*B*). EEA1 was mostly retained in phagosomes whereas TfR was nearly depleted during autophagosome accumulation induced by the drug. In contrast, CatD and LAMP1 were slightly downregulated under the same treatment. The differential effects of vinblastine on recruitment of the various endosomal and lysosomal proteins to phagosomes might reflect distinct trafficking routes of the proteins between autophagosomes and LBC phagosomes.

Conclusions

Proteomic analysis of a purified membrane fraction from LBC phagosomes resulted in the identification of many new proteins as well as clues regarding a relationship between phagocytosis and autophagy. The two types of phagocytic compartments involved in these processes, generated by seemingly different pathways, may undergo a direct fusion that allows them to exchange and degrade constituents. The molecular machinery underlying the putative fusion event would be of significant future interest. Autophagy is thought to facilitate the control and depletion of intracellular pathogens (39, 40). In this regard the process has a functional relationship with phagocytosis, whereby microbes from the external environment are internalized and digested. A potential synergy between autophagocytosis and conventional phagocytosis of pathogenic microbes warrants further investigation.

Acknowledgements

We thank Dr. Gregory Barton and Sarah Ewald for the kind gift of RAW cells stably expressing the TLR9-HA fusion protein, Dr. Patrick Fitzgerald for the generous offer of LC3-GFP-expressing RAW cells, Dr. Hu Cang for assistance with proteomic data analysis, and Dr. Qing Zhong for helpful discussions. This work was supported by a grant from the National Institutes of Health (AI51622) and the US Department of Energy. This work was supported by the U.S. Department of Energy under Contract No. DE-AC02-05CH11231.

References

1. Stuart, L. M. & Ezekowitz, R. A. (2005) *Immunity* **22,** 539-550.
2. Underhill, D. M. & Ozinsky, A. (2002) *Annual review of immunology* **20,** 825-852.
3. Jutras, I. & Desjardins, M. (2005) *Annual review of cell and developmental biology* **21,** 511-527.
4. Desjardins, M. & Griffiths, G. (2003) *Current opinion in cell biology* **15,** 498-503.
5. Garin, J., Diez, R., Kieffer, S., Dermine, J. F., Duclos, S., Gagnon, E., Sadoul, R., Rondeau, C., & Desjardins, M. (2001) *The Journal of cell biology* **152,** 165-180.
6. Rogers, L. D. & Foster, L. J. (2007) *Proceedings of the National Academy of Sciences of the United States of America* **104,** 18520-18525.
7. Jutras, I., Houde, M., Currier, N., Boulais, J., Duclos, S., Laboissiere, S., Bonneil, E., Kearney, P., Thibault, P., Paramithiotis, E.*, et al.* (2007) *Mol Cell Proteomics*.
8. Stuart, L. M., Boulais, J., Charriere, G. M., Hennessy, E. J., Brunet, S., Jutras, I., Goyette, G., Rondeau, C., Letarte, S., Huang, H.*, et al.* (2007) *Nature* **445,** 95-101.
9. Gotthardt, D., Blancheteau, V., Bosserhoff, A., Ruppert, T., Delorenzi, M., & Soldati, T. (2006) *Mol Cell Proteomics* **5,** 2228-2243.
10. Marion, S., Laurent, C., & Guillen, N. (2005) *Cellular microbiology* **7,** 1504-1518.
11. Mizushima, N., Levine, B., Cuervo, A. M., & Klionsky, D. J. (2008) *Nature* **451,** 1069-1075.
12. Shintani, T. & Klionsky, D. J. (2004) *Science (New York, N.Y* **306,** 990-995.
13. Levine, B. & Deretic, V. (2007) *Nature reviews* **7,** 767-777.
14. Desjardins, M., Celis, J. E., van Meer, G., Dieplinger, H., Jahraus, A., Griffiths, G., & Huber, L. A. (1994) *The Journal of biological chemistry* **269,** 32194-32200.
15. Gu, S., Chen, J., Dobos, K. M., Bradbury, E. M., Belisle, J. T., & Chen, X. (2003) *Mol Cell Proteomics* **2,** 1284-1296.
16. Peng, J., Elias, J. E., Thoreen, C. C., Licklider, L. J., & Gygi, S. P. (2003) *J Proteome Res* **2,** 43-50.
17. Harris, J., De Haro, S. A., Master, S. S., Keane, J., Roberts, E. A., Delgado, M., & Deretic, V. (2007) *Immunity* **27,** 505-517.
18. Rez, G., Csak, J., Fellinger, E., Laszlo, L., Kovacs, A. L., Oliva, O., & Kovacs, J. (1996) *European journal of cell biology* **71,** 341-350.
19. Stroikin, Y., Dalen, H., Loof, S., & Terman, A. (2004) *European journal of cell biology* **83,** 583-590.
20. Desjardins, M., Huber, L. A., Parton, R. G., & Griffiths, G. (1994) *The Journal of cell biology* **124,** 677-688.
21. Desjardins, M., Nzala, N. N., Corsini, R., & Rondeau, C. (1997) *Journal of cell science* **110 (Pt 18),** 2303-2314.
22. Claus, V., Jahraus, A., Tjelle, T., Berg, T., Kirschke, H., Faulstich, H., & Griffiths, G. (1998) *The Journal of biological chemistry* **273,** 9842-9851.
23. Scianimanico, S., Desrosiers, M., Dermine, J. F., Meresse, S., Descoteaux, A., & Desjardins, M. (1999) *Cellular microbiology* **1,** 19-32.
24. Duclos, S., Diez, R., Garin, J., Papadopoulou, B., Descoteaux, A., Stenmark, H., & Desjardins, M. (2000) *Journal of cell science* **113 Pt 19,** 3531-3541.
25. Grosshans, B. L., Ortiz, D., & Novick, P. (2006) *Proceedings of the National Academy of Sciences of the United States of America* **103,** 11821-11827.
26. Chen, Y. A. & Scheller, R. H. (2001) *Nat Rev Mol Cell Biol* **2,** 98-106.
27. Steegmaier, M., Klumperman, J., Foletti, D. L., Yoo, J. S., & Scheller, R. H. (1999) *Molecular biology of the cell* **10,** 1957-1972.
28. Tran, T. H., Zeng, Q., & Hong, W. (2007) *Journal of cell science* **120,** 1028-1041.
29. Barton, G. M. (2007) *Seminars in immunology* **19,** 33-40.

30. Bagshaw, R. D., Mahuran, D. J., & Callahan, J. W. (2005) *Mol Cell Proteomics* **4,** 133-143.
31. Schindler, C., Levy, D. E., & Decker, T. (2007) *The Journal of biological chemistry* **282,** 20059-20063.
32. Behrmann, I., Smyczek, T., Heinrich, P. C., Schmitz-Van de Leur, H., Komyod, W., Giese, B., Muller-Newen, G., Haan, S., & Haan, C. (2004) *The Journal of biological chemistry* **279,** 35486-35493.
33. Kabeya, Y., Mizushima, N., Ueno, T., Yamamoto, A., Kirisako, T., Noda, T., Kominami, E., Ohsumi, Y., & Yoshimori, T. (2000) *The EMBO journal* **19,** 5720-5728.
34. Levine, B. & Klionsky, D. J. (2004) *Developmental cell* **6,** 463-477.
35. Petiot, A., Pattingre, S., Arico, S., Meley, D., & Codogno, P. (2002) *Cell structure and function* **27,** 431-441.
36. Petiot, A., Ogier-Denis, E., Blommaart, E. F., Meijer, A. J., & Codogno, P. (2000) *The Journal of biological chemistry* **275,** 992-998.
37. Kabeya, Y., Mizushima, N., Yamamoto, A., Oshitani-Okamoto, S., Ohsumi, Y., & Yoshimori, T. (2004) *Journal of cell science* **117,** 2805-2812.
38. Fratti, R. A., Chua, J., Vergne, I., & Deretic, V. (2003) *Proceedings of the National Academy of Sciences of the United States of America* **100,** 5437-5442.
39. Gutierrez, M. G., Master, S. S., Singh, S. B., Taylor, G. A., Colombo, M. I., & Deretic, V. (2004) *Cell* **119,** 753-766.
40. Alonso, S., Pethe, K., Russell, D. G., & Purdy, G. E. (2007) *Proceedings of the National Academy of Sciences of the United States of America* **104,** 6031-6036.

Figure Legends

Figure 1. Macrophage subcellular fractionation of phagosomal membranes and proteomic analyses. The blue band on top of the sucrose gradient is the LBC phagosome, and fractions 1, 2, 3 represent subcellular fractions below the phagosome band.

Figure 2. Immunoblot analysis of subcellular fractions. (A) Blot probed for certain organelle markers. (B) Blot probed for membrane-bound endosomal markers and a lysosomal hydrolase. Fractions are denoted in Fig. 1. “No beads” indicates a sample taken from the same position occupied by LBC phagosomes in the sucrose gradient, yet derived from macrophages without beads. Each lane was loaded with 3 μg of total protein and equal loading was verified by silver stain (see SI Fig. S1).

Figure 3. Comparison of this membrane-enriched phagosome proteomic data to the reported total phagosome proteomic data. (A) Venn diagram of total protein IDs from this membrane proteomic dataset and Foster’s comprehensive proteomic dataset[6] for LBC phagosomes. (B) Histogram of predicted molecular weights of the proteins in the two datasets. (C) Histogram of the number of predicted transmembrane helices (TMH) in the unique proteins identified in the two datasets. Unique IDs refers to proteins exclusively reported in one dataset.

Figure 4. Functional categorization of the 546 proteins identified in the phagosomal membrane fraction. “Others” combines four small groups: cell adhesion, nucleotide metabolism, protein folding and apoptosis. The detailed classification of each protein is shown in SI Table S3.

Figure 5. Immunoblots of newly found proteins in phagosomal membranes. A portion of each subcellular fraction was separated by SDS-PAGE and analyzed by Western blot probing for VAMP4, LC3, JAK1, TLR7 and TLR9. TCL+ = total cell lysate obtained from RAW cells expressing HA-tagged TLR9; TCL- = total cell lysate from normal RAW cells. Anti-HA was used to probe for TLR9 expression.

Figure 6. Regulation of phagosomal proteins in response to autophagy induction. Immunoblots of (A) newly found phagosomal components and (B) endosomal markers in either macrophage total cell lysate (TCL) (left) or phagosomal extracts (right). Macrophages were subjected to treatment with rich medium (lane 1 and 6), starvation (lane 2 and 7), starvation and 10 mM 3-methyladenine (3-MA) (lane 3 and 8),

starvation and 50 μM vinblastine (VIN) (lane 4 and 9), starvation and protease inhibitors (INH) (lane 5 and 10). The loading control was tubulin for macrophage TCL and actin for phagosome extracts.

Figure 7. Translocation of GFP-LC3 to LBC phagosomes during autophagy induction. RAW cells stably expressing GFP-LC3 were allowed to internalize latex beads (3 μm) for 1 h, and then incubated with medium containing lysosomal protease inhibitor chloroquine (50 μM), EBSS buffer alone, EBSS containing 3-MA (10 mM) for 2 h. Control was treated with rich medium after bead internalization. LysoTracker was added in the last 15 min to stain acidic vacuoles. All cells were treated while alive with nuclear stain Hoechst 33342 (blue). Shown are representative images of different samples. Scale bar = 5 μm.

Supporting Information

Fig. S1. SDS-PAGE analysis of proteins extracted from subcellular fractions collected as shown in Fig. 1. Each lane was loaded with 3 μg of total protein.

Fig. S2. . Immunoblot analysis of organelle markers in subcellular fractions isolated from macrophages subjected to (A) starvation buffer (EBSS); (B) starvation buffer with 3-MA (C) starvation buffer with vinblastine. Fractions are denoted in Fig. 1 and Fig. 2. See Experimental Procedures for details for drug treatment. Each lane was loaded with 3 μg of total protein.

Table S1. Mascot results listing proteins identified in phagosomal membrane proteome.

Table S2. Predicted molecular weights and numbers of helical domains of proteins from two datasets. The unique IDs from each dataset are highlighted.

Table S3. Functional grouping of each protein identified in this phagosomal membrane proteomic study.

Table S4. Relative abundance of phagosomal membrane proteins indicated by Mascot results

Table 1. Identification of TLR family members in the membrane proteome of LBC phagosomes

Protein Name	IPI accession no.	Major ligands in innate immunity	Predicted protein MW	Mascot Score of Protein ID	No. of peptide IDs	Relative abundance index*
TLR 2	IPI00131898	Lipids and glycans from bacteria and fungi	91 KD	152	6	3.6
TLR 3	IPI00320618	dsRNA from viruses	104 KD	108	4	3.8
TLR 7	IPI00122181	ssRNA from viruses	123 KD	897	47	38
TLR 9	IPI00318748	DNA from viruses and bacteria	118 KD	146	10	8.5
TLR 13	IPI00342691	Unknown	115 KD	1160	52	45

* Calculated by dividing “No. of peptide IDs” with “Predicted protein MW”, then multiplying by 100.

Fig. 1

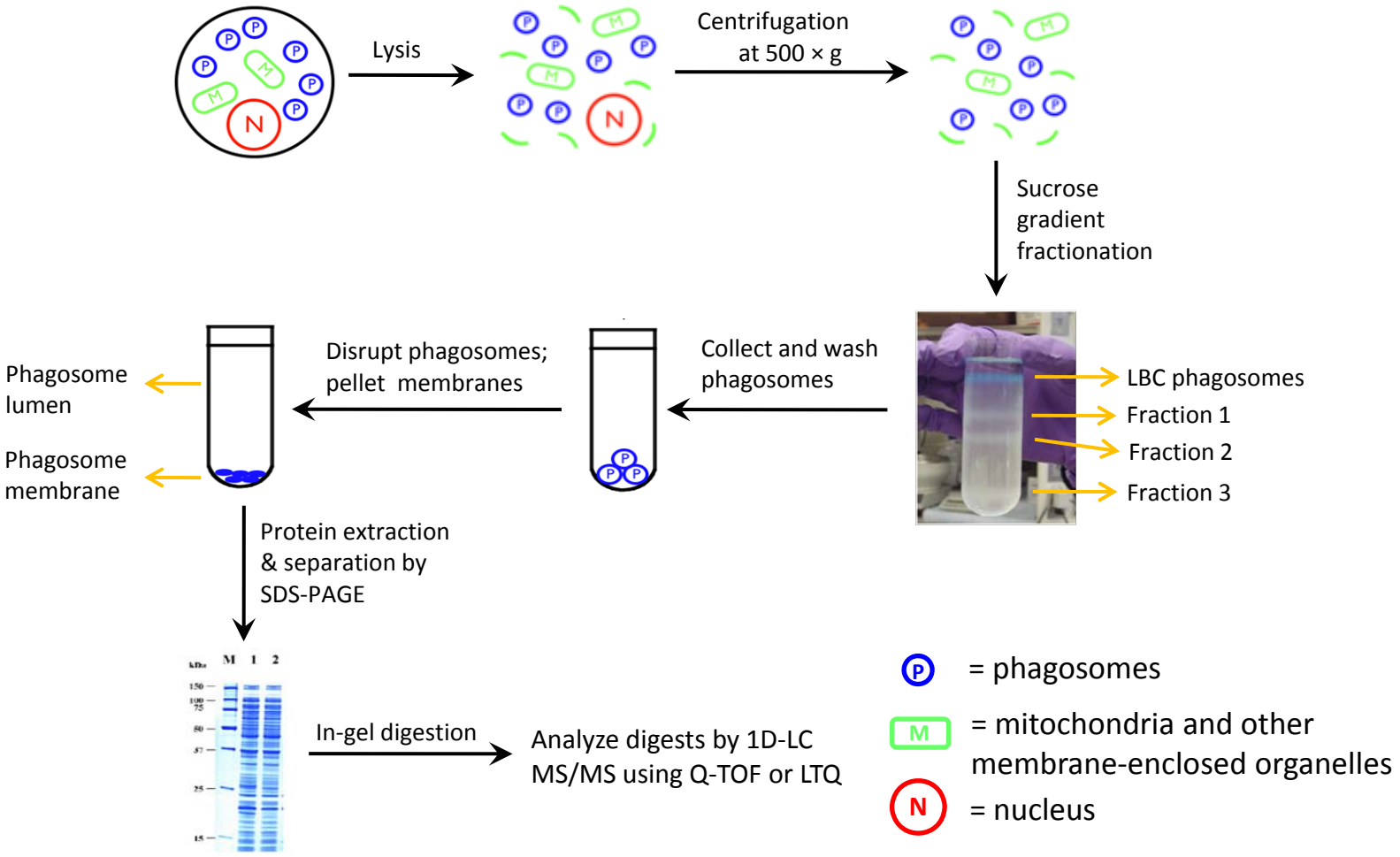
Lysis
Centrifugation
at 500 × g
Sucrose
gradient
fractionation
LBC phagosomes
Fraction 1
Fraction 2
Fraction 3
Collect and wash
phagosomes
Disrupt phagosomes;
pellet membranes
Phagosome
lumen
Phagosome
membrane
Protein extraction
& separation by
SDS-PAGE
M 1 2
In-gel digestion
Analyze digests by 1D-LC
MS/MS using Q-TOF or LTQ
= phagosomes
= mitochondria and other
membrane-enclosed organelles
= nucleus

Fig. 2*A*

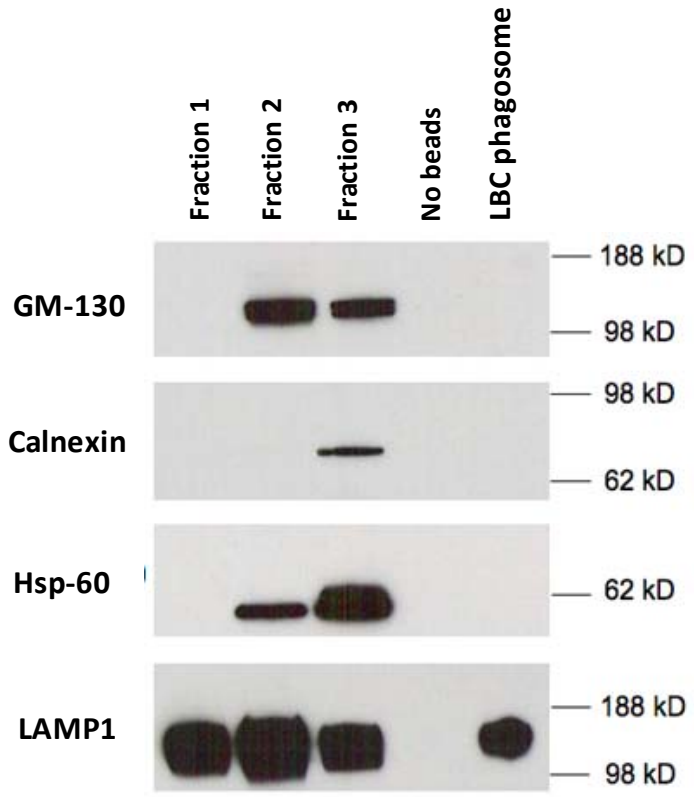
Fraction 1
Fraction 2
Fraction 3
No beads
LBC phagosome
GM-130
188 kD
98 kD
Calnexin
98 kD
62 kD
Hsp-60
62 kD
LAMP1
188 kD
98 kD

Fig. 2*B*

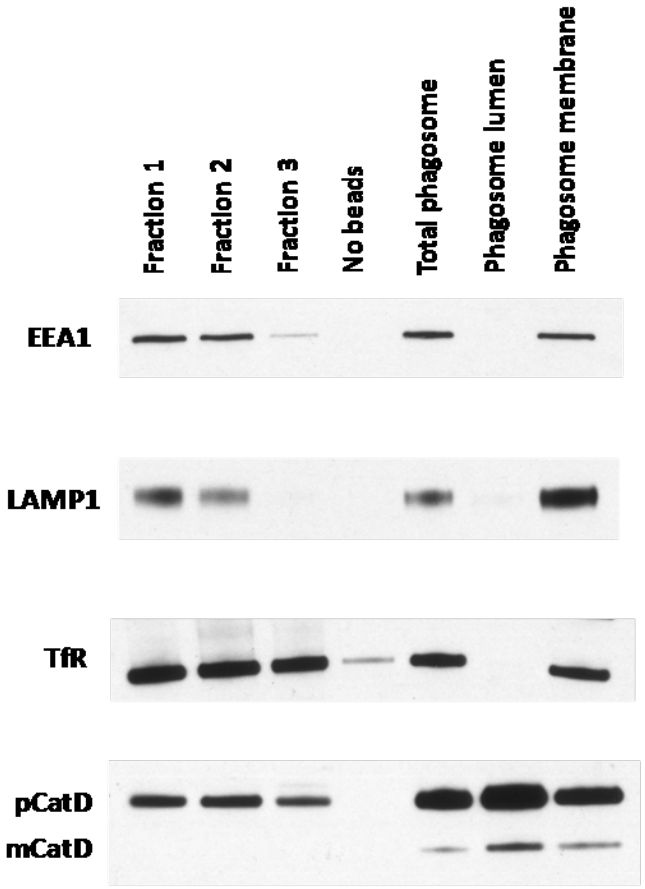
Fraction 1
Fraction 2
Fraction 3
No beads
Total phagosome
Phagosome lumen
Phagosome membrane
EEA1
LAMP1
TfR
pCatD
mCatD

Fig. 3

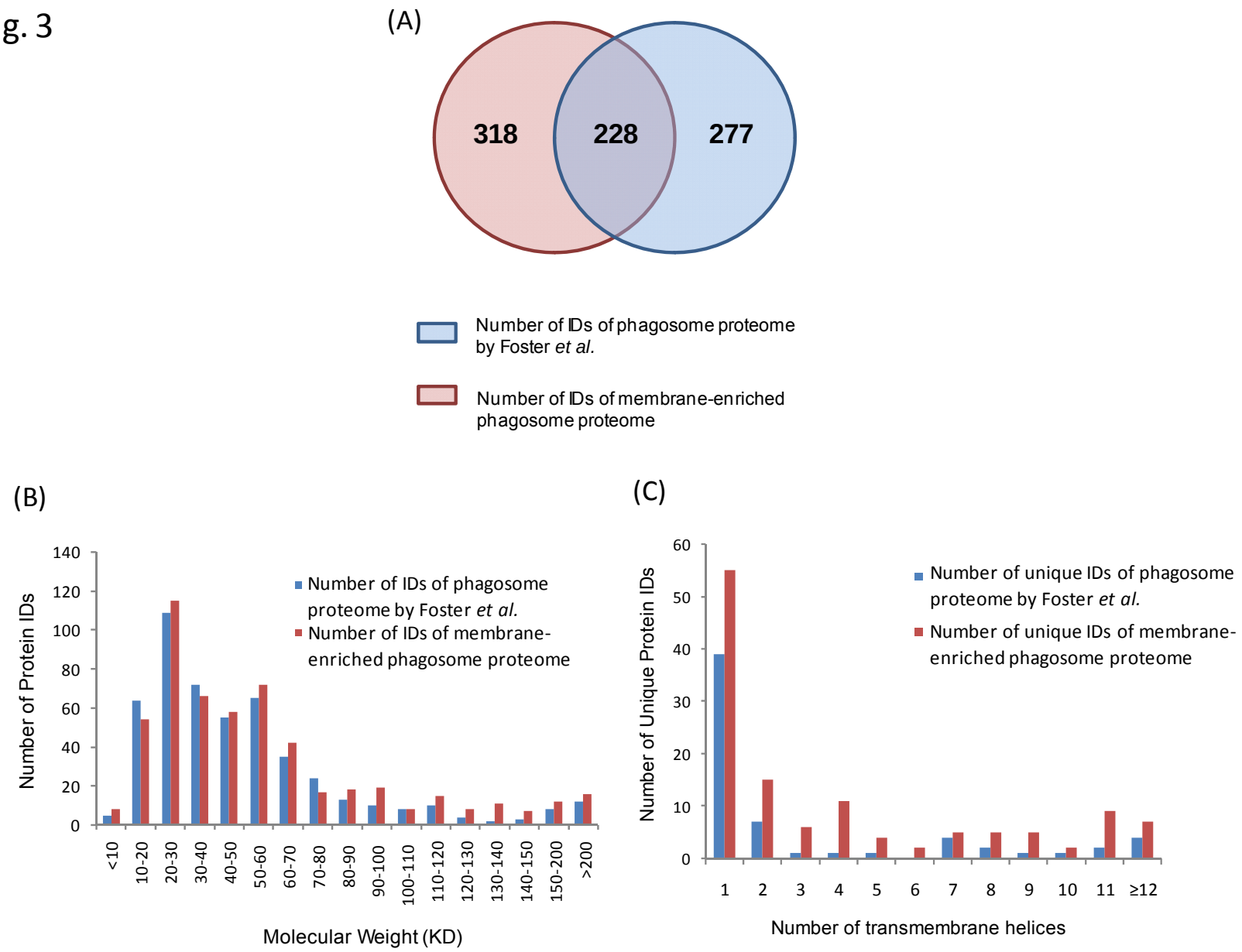
(A)
318
228
277
Number of IDs of phagosome proteome by Foster et al.
Number of IDs of membrane-enriched phagosome proteome
(B)
Number of Protein IDs
140
120
100
80
60
40
20
0
Number of IDs of phagosome proteome by Foster et al.
Number of IDs of membrane-enriched phagosome proteome
<10
10-20
20-30
30-40
40-50
50-60
60-70
70-80
80-90
90-100
100-110
110-120
120-130
130-140
140-150
150-200
>200
Molecular Weight (KD)
(C)
Number of Unique Protein IDs
60
50
40
30
20
10
0
Number of unique IDs of phagosome proteome by Foster et al.
Number of unique IDs of membrane-enriched phagosome proteome
1
2
3
4
5
6
7
8
9
10
11
≥12
Number of transmembrane helices

Fig. 4

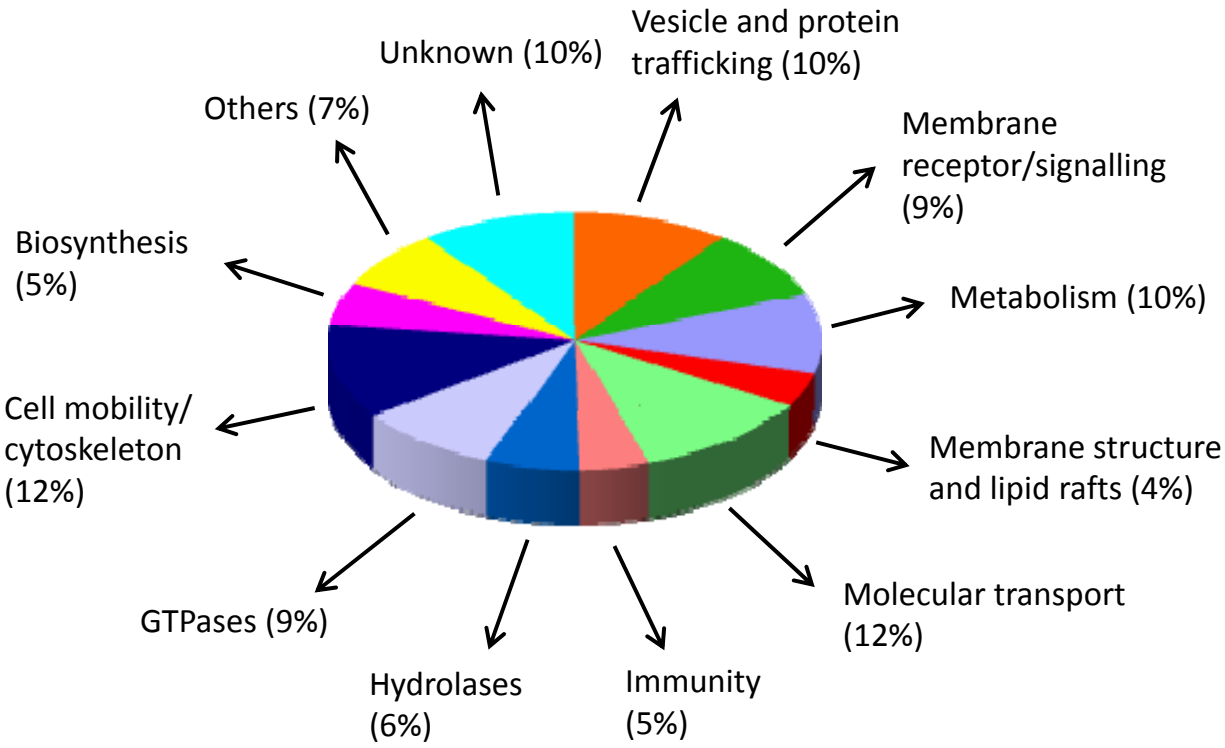
Unknown (10%)
Vesicle and protein trafficking (10%)
Others (7%)
Membrane receptor/signalling (9%)
Biosynthesis (5%)
Metabolism (10%)
Cell mobility/ cytoskeleton (12%)
Membrane structure and lipid rafts (4%)
GTPases (9%)
Molecular transport (12%)
Hydrolases (6%)
Immunity (5%)

Fig. 5

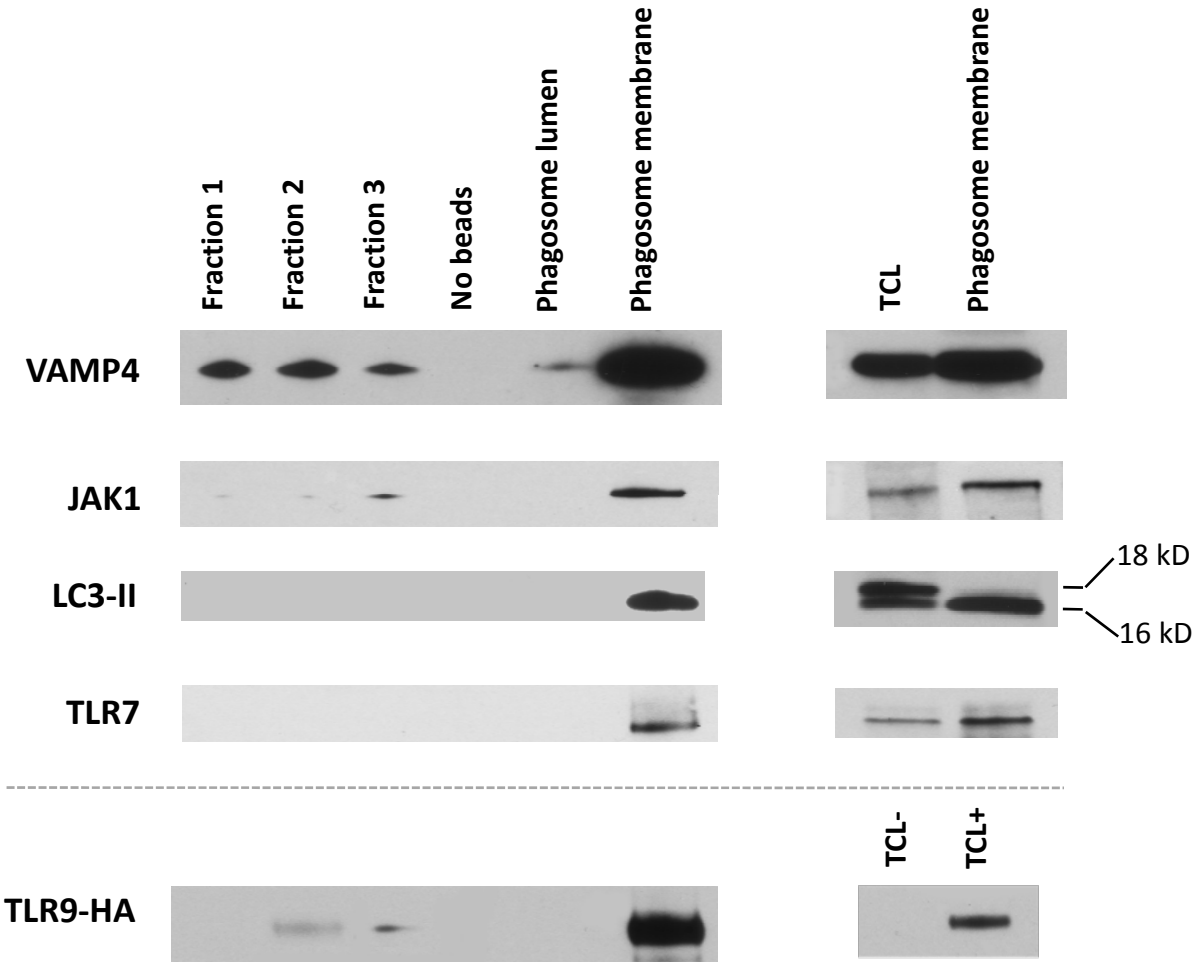
Fraction 1
Fraction 2
Fraction 3
No beads
Phagosome lumen
Phagosome membrane
TCL
Phagosome membrane
VAMP4
JAK1
LC3-II
18 kD
16 kD
TLR7
TCL-
TCL+
TLR9-HA

Fig. 6*A*

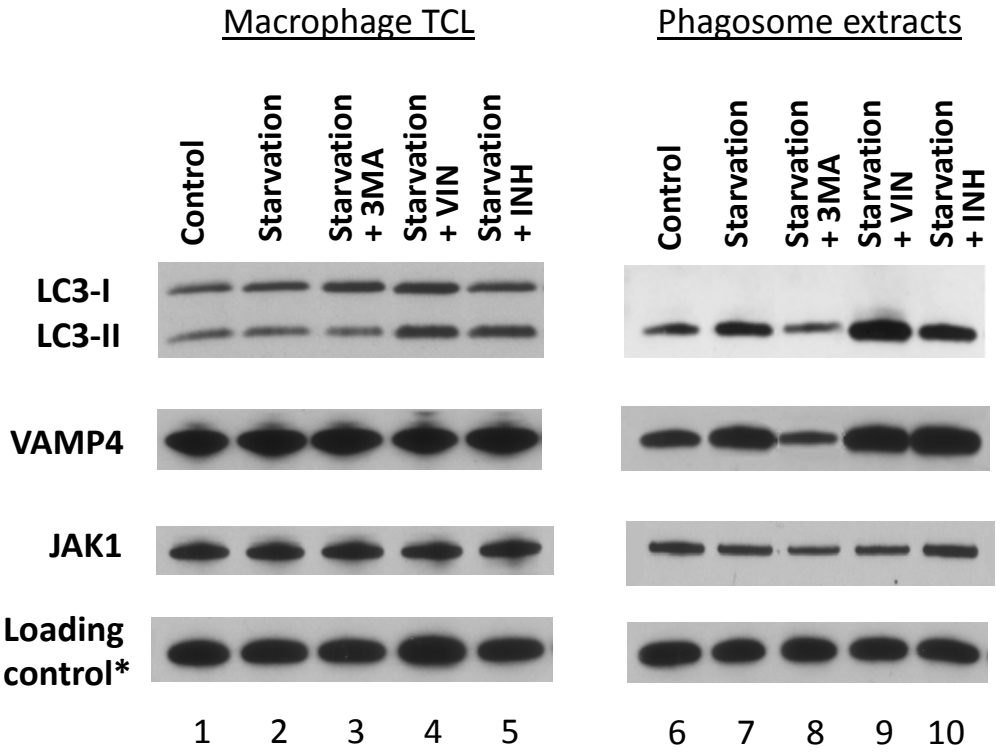
Macrophage TCL
Phagosome extracts
Control
Starvation
Starvation + 3MA
Starvation + VIN
Starvation + INH
Control
Starvation
Starvation + 3MA
Starvation + VIN
Starvation + INH
LC3-I
LC3-II
VAMP4
JAK1
Loading control*
1 2 3 4 5 6 7 8 9 10

Fig. 6*B*

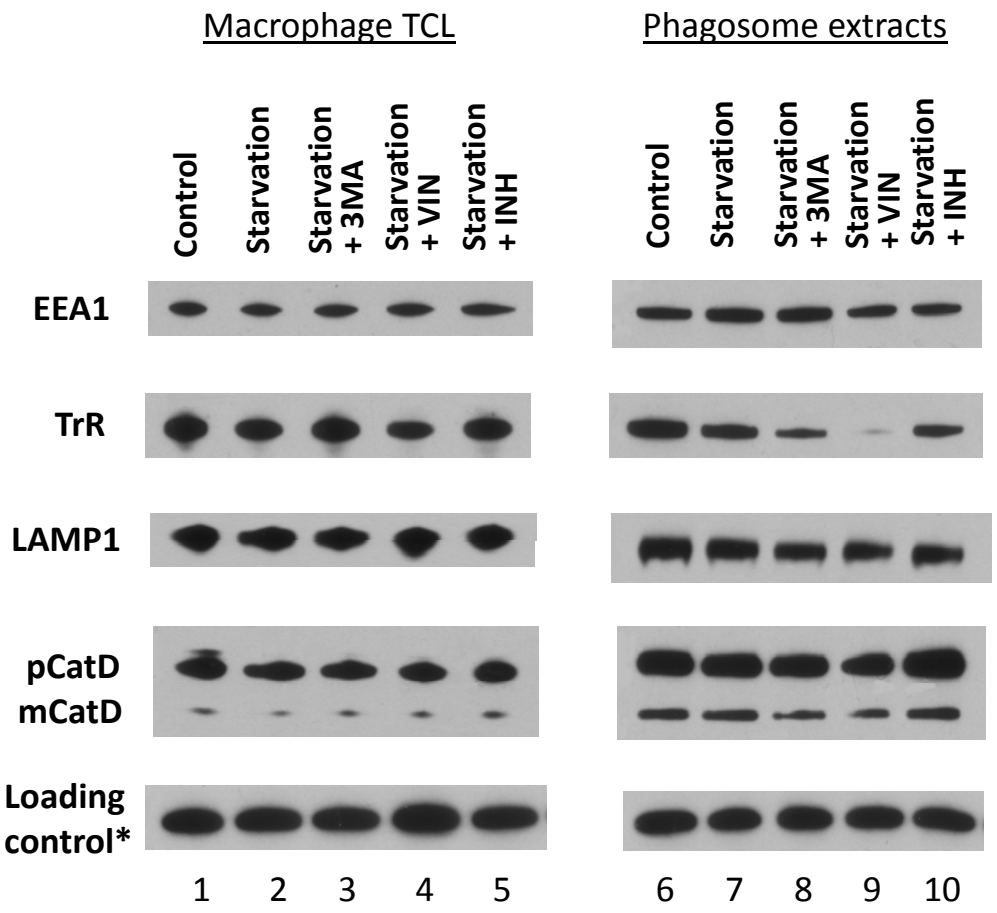
Macrophage TCL
Phagosome extracts
Control
Starvation
Starvation + 3MA
Starvation + VIN
Starvation + INH
Control
Starvation
Starvation + 3MA
Starvation + VIN
Starvation + INH
EEA1
TrR
LAMP1
pCatD
mCatD
Loading control*
1 2 3 4 5 6 7 8 9 10

Fig. 7

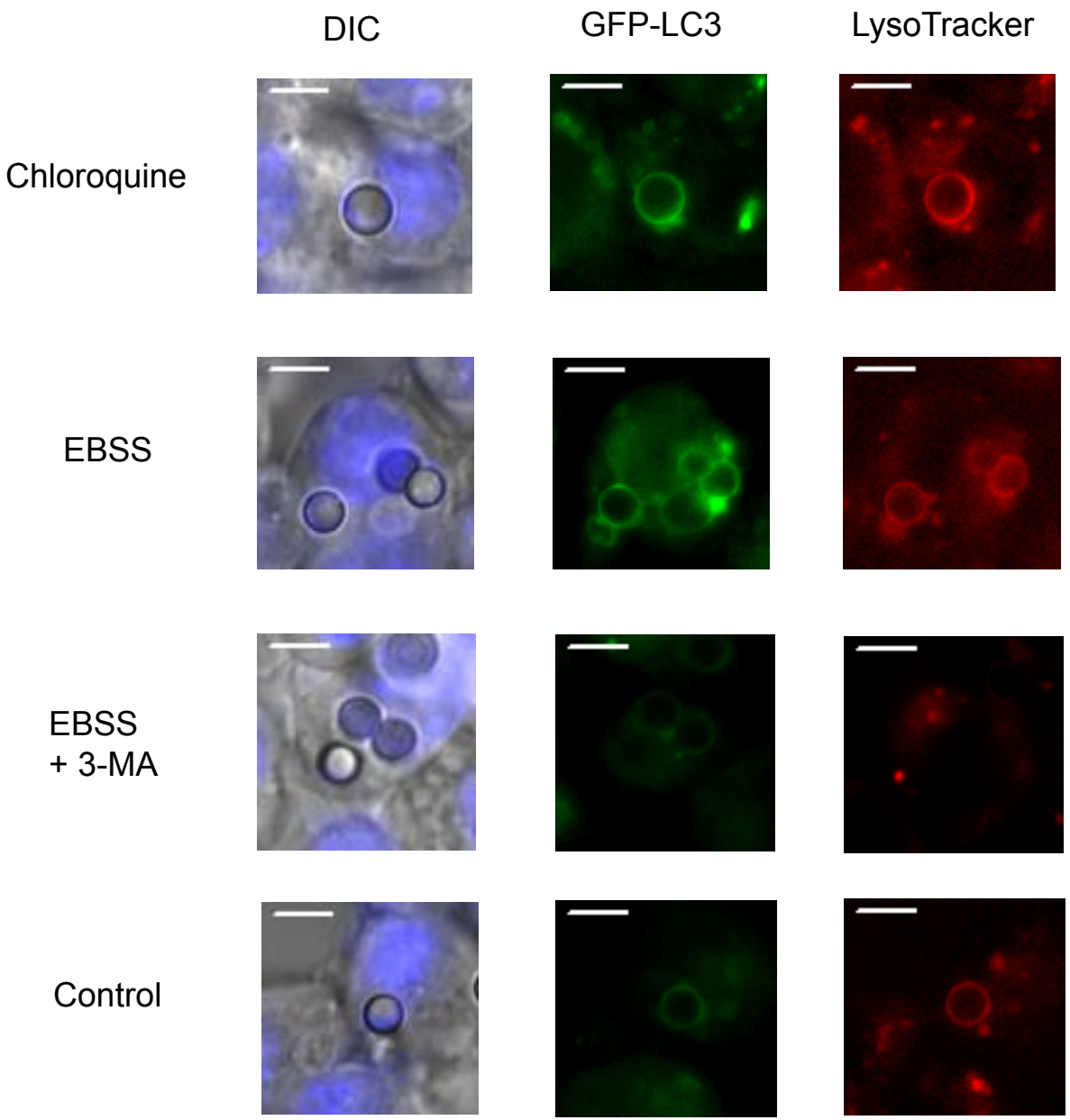

SI Fig. S1

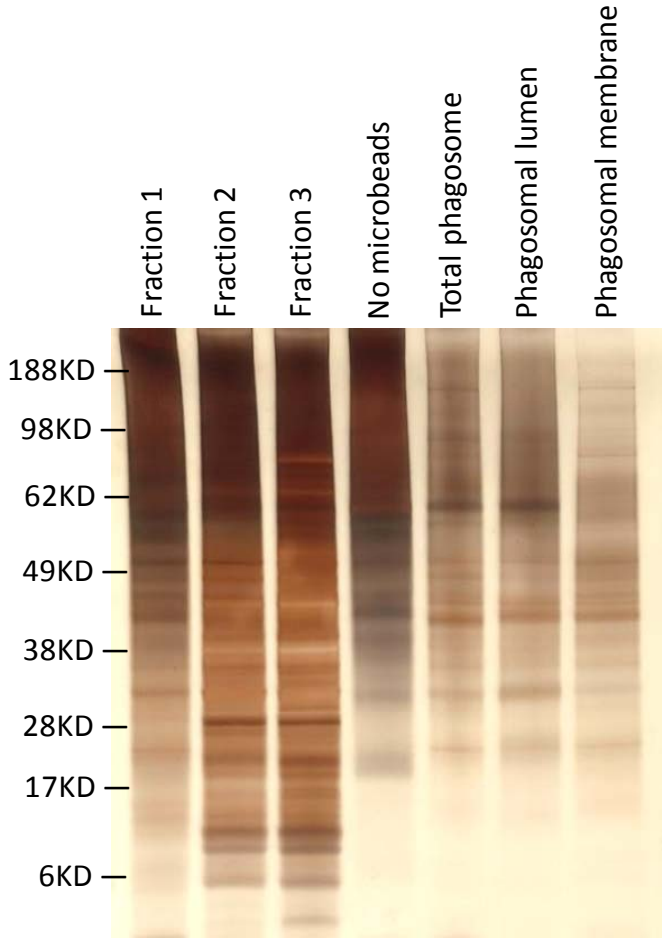
Fraction 1
Fraction 2
Fraction 3
No microbeads
Total phagosome
Phagosomal lumen
Phagosomal membrane
188KD
98KD
62KD
49KD
38KD
28KD
17KD
6KD

SI Fig. S2

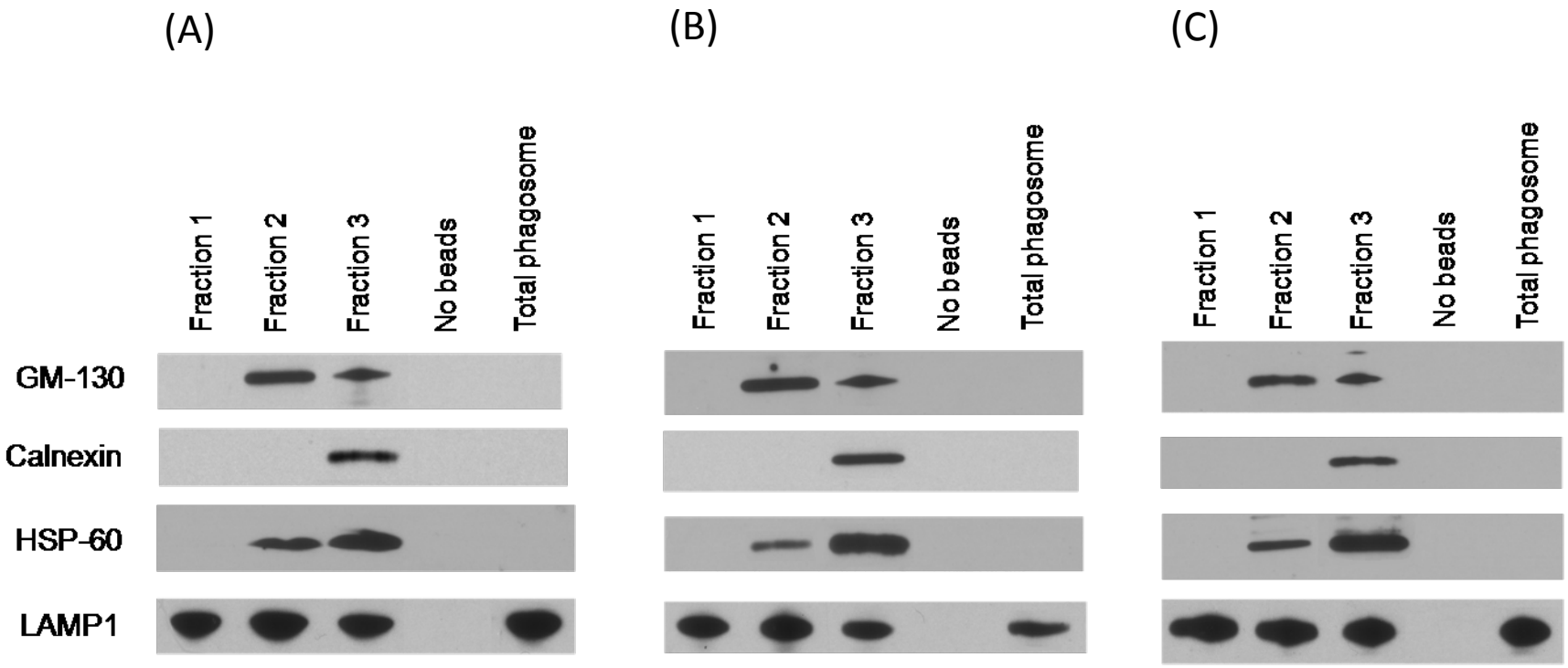
(A)
(B)
(C)
Fraction 1
Fraction 2
Fraction 3
No beads
Total phagosome
GM-130
Calnexin
HSP-60
LAMP1